

Article

Poly(3,4-Ethylenedioxythiophene) Nanoparticles as Building Blocks for Hybrid Thermoelectric Flexible Films

Jose F. Serrano-Claumarchirant ¹, Mario Culebras ², Andrés Cantarero ³, Clara M. Gómez ^{1,*}  and Rafael Muñoz-Espí ^{1,*} 

¹ Institute of Materials Science (ICMUV), University of Valencia, 46980 Paterna, Spain; j.francisco.serrano@uv.es

² Stokes Laboratories, Bernal Institute, University of Limerick, V94 T9PX Limerick, Ireland; mario.culebrasrubio@ul.ie

³ Institute of Molecular Science (ICMol), University of Valencia, 46980 Paterna, Spain; andres.cantarero@uv.es

* Correspondence: clara.gomez@uv.es (C.M.G.); rafael.munoz@uv.es (R.M.-E.); Tel.: +34-9635-44210 (R.M.-E.)

Received: 4 December 2019; Accepted: 24 December 2019; Published: 28 December 2019



Abstract: Hybrid thermoelectric flexible films based on poly(3,4-ethylenedioxythiophene) (PEDOT) nanoparticles and carbon nanotubes were prepared by using layer-by-layer (LbL) assembly. The employed PEDOT nanoparticles were synthesized by oxidative miniemulsion polymerization by using iron(III) *p*-toluenesulfonate hexahydrate (FeTos) as an oxidant and poly(diallyldimethylammonium chloride) (PDADMAC) as stabilizer. Sodium deoxycholate (DOC) was used as a stabilizer to prepare the aqueous dispersions of the carbon nanotubes. Hybrid thermoelectric films were finally prepared with different monomer/oxidant molar ratios and different types of carbon nanotubes, aiming to maximize the power factor (PF). The use of single-wall (SWCNT), double-wall (DWCNT), and multiwall (MWCNT) carbon nanotubes was compared. The Seebeck coefficient was measured by applying a temperature difference between the ends of the film and the electrical conductivity was measured by the Van der Pauw method. The best hybrid film in this study exhibited a PF of $72 \mu\text{W m}^{-1}\text{K}^{-2}$. These films are prepared from aqueous dispersions with relatively low-cost materials and, due to lightweight and flexible properties, they are potentially good candidates to recover waste heat in wearable electronic applications.

Keywords: PEDOT; nanoparticles; carbon nanotubes; hybrid material; thermoelectricity; miniemulsion; layer-by-layer assembly; electrical conductivity

1. Introduction

Most of the energy produced today comes from classical energy sources, which are unfortunately non-renewable and generate many environmental problems. There is, therefore, a serious need to look for more sustainable and environmentally friendly sources. Thermoelectric generators can significantly contribute to this purpose, recovering energy from waste heat. In the last decade, thermoelectric materials have been attracting great interest in the field of energy harvesting [1]. The thermoelectric efficiency is determined by the dimensionless figure of merit, ZT , given by the expression $ZT = S^2\sigma T/\kappa$, where S , σ , and κ are the Seebeck coefficient, electrical conductivity, and thermal conductivity, respectively. Thermoelectric materials should not only be highly efficient, but also low-cost, manufacturing-scalable, and eco-friendly. Traditionally, the use of inorganic semiconductors has dominated thermoelectric applications. However, their inherent problems, such as toxicity, scarcity of raw materials, and high production cost, have motivated the search of new materials capable to overcome such problems [2]. Because of their promising values of thermoelectric efficiency, conducting

polymer nanocomposites and hybrids can be a real alternative to typical inorganic semiconductors based, for instance, on Bi_2Te_3 [3–5]. Conducting polymers based on poly(3, 4-ethylenedioxythiophene) (PEDOT) have shown efficient values of ZT in the range from 0.1 to 0.4 [1,6,7]. On the other hand, carbon nanotubes (CNTs) have been shown to be good nanofillers to develop high efficient thermoelectric nanocomposites, reaching very high values of power factor (PF), defined as $PF = S^2 \sigma$ [8–10]. It is known that the electrical properties of conducting polymers depend significantly on the arrangement of the polymer chains [11–13]. Since CNTs are rolled graphene sheets, π – π interactions can occur between the graphene ring of the carbon nanotube and the aromatic ring or double bonds of the conducting polymer, which can act as a template for an optimal ordering and, thus, produce a synergistic effect on thermoelectric properties [14]. In addition, the combination of conducting polymer and inorganic semiconductor-based on Te and Bi_2Te_3 has demonstrated an enormous potential in terms of thermoelectric efficiency, being in some of the cases even higher than for the starting materials [15,16].

Multilayered materials based on conducting polymers and carbon nanostructures (CNTs and graphene) stand out over the rest because their thermoelectric efficiency can be higher than bulk Bi_2Te_3 . For example, very high power factors have been obtained for multilayered thin films prepared using layer-by-layer (LbL) assembly and based on polyaniline (PANI), double-walled carbon nanotubes (DWCNT) and graphene ($1750 \mu\text{W m}^{-1}\text{K}^{-2}$), or PANI, DWCNT, poly(3,4-ethylenedioxythiophene)/poly(styrene sulfonate) (PEDOT:PSS), and graphene ($2710 \mu\text{W m}^{-1}\text{K}^{-2}$) [17,18]. LbL assembly also allows the preparation of n-type thermoelectric materials, as previously reported for the system PEI–DWCNTs/PVP-graphene (PEI: polyetherimide, PVP: polyvinylpyrrolidone) [19]. Although there is no doubt about the interest of this kind of layered materials, the lack of studies on their thermoelectric properties highlights the need for more research to open the gate to a new generation of highly efficient organic thermoelectric materials.

Additionally to the stated above, flexible thermoelectric materials have also attracted interest for their use in wearable devices, in which the body temperature can be used to obtain energy. When using inorganic materials, high power factor were obtained, for instance, for n-type and p-type Sb_2Te_3 by electrochemical deposition (-80 and $100 \mu\text{W m}^{-1}\text{K}^{-2}$, respectively) [20,21]. However, conducting polymers are much more flexible than inorganic materials and offer the possibility to produce highly flexible films for thermoelectric applications [22] in different substrates, such as paper with PEDOT:PSS [23,24] or polyimide with poly(3-hexylthiophene-2,5-diyl) (P3HT)/CNT nanocomposites [25].

In this work, we have prepared films from PEDOT nanoparticles, which embed single-wall (SWCNT), double-wall (DWCNT), and multiwall (MWCNT) carbon nanotubes. We analyze the effect of different types of CNTs on the thermoelectric properties. The use of PEDOT nanoparticles allows us to tune the electrical properties and the surface charge, which can be influenced by experimental parameters, such as the nature of the stabilizer used during nanoparticle synthesis (nonionic, cationic or anionic) or the oxidant concentration.

2. Experimental Section

2.1. Materials

Poly(diallyldimethylammonium chloride) (PDADMAC, 20 wt.% in water), iron(III) *p*-toluenesulfonate hexahydrate (FeTos) and sodium deoxycholate (DOC, $\geq 97\%$ by titration) were purchased from Sigma-Aldrich. 3, 4-Ethylenedioxythiophene (EDOT) 97% was obtained from Alfa Aesar. Hydrogen peroxide 30 wt.% was purchased from PanReac AppliChem (Barcelona, Spain). Multiwalled carbon nanotubes (MWCNTs, 12–15 nm outer and 4 nm inner wall diameter, $> 1 \mu\text{m}$ length, $C \geq 95 \text{ wt}\%$) were obtained from Bayer MaterialScience (Leverkusen, Germany). Double-walled carbon nanotubes (DWCNTs, 2–4 nm outer and 1–3 nm inner wall diameter, $> 50 \mu\text{m}$ length, $C > 60\%$) and single-walled carbon nanotubes (SWCNTs, 1–2 nm wall diameter, 5–30 μm length, $C = 90\%$) were purchased from Nanostructured & Amorphous Materials, Inc. (Houston, TX, USA). Polyethylene

terephthalate (PET), with a thickness of 179 μm (trade name ST 505 by DuPont Teijin, purchased from Tekra Corp, New Berlin, WI, USA) were rinsed with deionized water, methanol, and deionized water again, and dried with filtered air before use. Corona treatment (a BD-20C Corona Treater, Electro-Technic Products Inc., Chicago, IL, USA) was used to improve adhesion of the first layer by oxidizing the polymer surface.

2.2. Synthesis of PEDOT Nanoparticles

The synthesis of PEDOT nanoparticles was carried out by chemical oxidation polymerization in miniemulsion, using FeTos as an oxidizer and PDADMAC as a stabilizer. First, the commercial PDADMAC aqueous solution (20 wt.%) was diluted in 40 mL of water and then EDOT was added and stirred at 800 rpm for 5 min. To obtain the miniemulsion, the mixture was ultrasonicated with the aid of a Branson Sonifier 450 (1/2 inch tip, amplitude of 70%, pulse of 90% for 10 min). The polymerization was carried out by slowly adding to the miniemulsion a solution of FeTos in 10 mL of water, according to the proportions shown in Table 1. Afterward, hydrogen peroxide was added. The samples were purified by centrifugation at 13,000 rpm for 20 min, which was repeated 3 times by discarding the supernatant. The purified samples were redispersed in 40 mL of water.

Table 1. Quantities of reagents used for the preparation of the nanoparticles shown in this work.

Molar Ratio EDOT:FeTos	PDADMAC (wt.%)	EDOT (M)	FeTos (M)	H ₂ O ₂ (M)
1:1	0.5	0.037	0.037	0.001
1:1.5	0.5	0.037	0.056	0.001
1:2	0.5	0.037	0.075	0.001

2.3. Film Preparation

Carbon nanotubes (0.05 wt.%) were dispersed in an aqueous solution of DOC (0.1 wt.%). The CNT suspensions were placed in an ultrasound bath for 30 min, followed by 20 min of ultrasonication with a Branson Sonifier 450 (1/2 inch tip, 70% amplitude, continuous mode), while cooling in an ice bath. Finally, the suspensions were placed for 30 min in the ultrasound bath. CNT dispersions were then centrifuged at 4000 rpm for 5 min to discard the nonstabilized CNTs. The assembly of PEDOT nanoparticles and CNT layers was carried out by using the layer-by-layer (LbL) technique via dip coating on a pre-treated polyethylene terephthalate (PET) substrate to improve film adhesion [26]. PET substrates were immersed in a cationic PEDOT: PDADMAC suspension for 5 min, followed by 3 washing steps of dipping in water, immersion in the anionic CNT:DOC suspension for 5 min, and eventually 3 further steps of washing in water. This process results in one deposition sequence of a PEDOT: PDADMAC–CNT:DOC bilayer (bL). This cycle was repeated to deposit the desired number of bilayers. Deposited multilayer films were washed and air-dried overnight, and then stored in a desiccator prior to further processing or characterization. The process of formation of the nanoparticles and the subsequent films is schematically depicted in Figure 1.

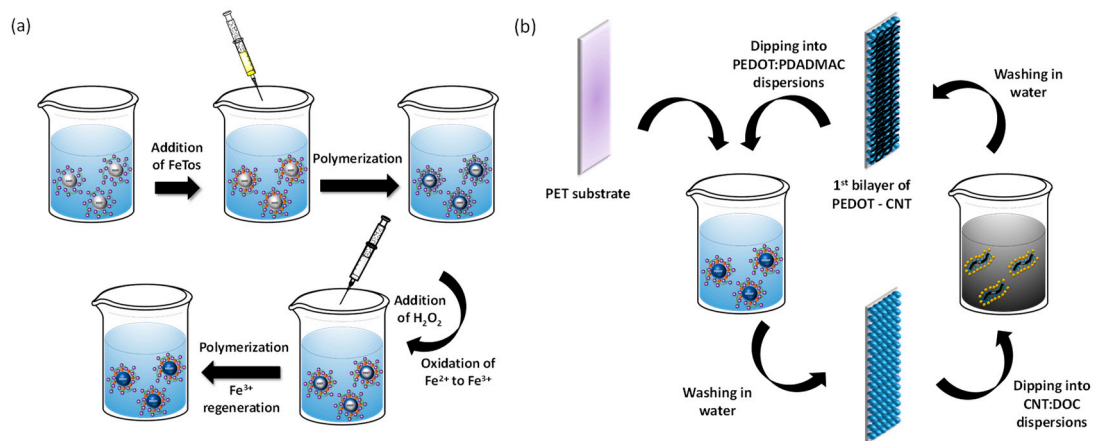


Figure 1. (a) Scheme of the polymerization of EDOT in miniemulsion and (b) scheme of the assembly of PEDOT nanoparticles and CNT.

2.4. Characterization Techniques

The morphological characterization of PEDOT nanoparticles was carried out by transmission electron microscopy (TEM) at an accelerating voltage of at 100 kV in a JEOL JEM-1010 microscope (JEOL Ltd., Japan, coupled with a digital camera MegaView III (GEMSIS GmbH, Germany). Zeta potential measurements of PEDOT:PDADMAC and CNT:DOC suspensions were measured in a Zetasizer Nano ZS (Malvern Instruments), diluting previously the samples in KCl 0.3 M (aqueous solution). Particle size of PEDOT:PDADMAC suspensions was measured by dynamic light scattering (Zetasizer Nano ZS).

The thickness of PEDOT–CNT films was measured by using a profilometer (Dektak 150, Veeco, USA). Reported values represent an average of at least 5 separate measurements of each film. Morphological characterization of the films was carried out by scanning electron microscopy (SEM) by using a Hitachi S-4800 microscope at an accelerating voltage of 20 kV and a working distance of 14 mm for palladium–gold coated surfaces. TEM was also conducted for samples prepared by embedding a small piece of coated PET in Durcupan ACM resin (Sigma-Aldrich), curing overnight, and then cutting cross-sections using an Ultra 45° diamond knife (Diatome, Hatfield, PA). These samples were imaged by using copper grids with the same equipment and accelerating voltage as for the nanoparticles.

For the electrical characterization, four contacts with silver paint were coated on the film surface. The electrical conductivity was measured with a Keithley 2400 SourceMeter equipment by using the Van der Pauw equation:

$$e^{-\pi \cdot d \cdot R_1 \sigma} + e^{-\pi \cdot d \cdot R_2 \sigma} = 1 \quad (1)$$

where d is the thickness of the film, R_1 and R_2 are the electrical resistance along a vertical and horizontal edges, respectively, and σ is the electrical conductivity.

The Seebeck coefficient is determined as the ratio between the electrical potential, ΔV , and the temperature difference, ΔT :

$$S = \frac{\Delta V}{\Delta T} \quad (2)$$

The electrical potential was measured with an Agilent 34401 A digital multimeter and the temperature difference was measured using PT100 resistors connected to a Lakeshore 340 temperature controller.

3. Results and Discussion

PEDOT nanoparticles were synthesized by chemical oxidation polymerization in miniemulsion with PDADMAC as a stabilizer, as schematically shown in Figure 1a. During the polymerization of EDOT in miniemulsion, different stages occur. After ultrasonication, EDOT droplets are stabilized by

PDADMAC. The observations suggest that when FeTos is added, iron(III) ions move to the EDOT–water interface and may partially oxidize EDOT to PEDOT, resulting in a PEDOT shell. As a consequence, iron (III) ions are reduced to iron(II). Finally, the addition of hydrogen peroxide oxidizes iron(II) to iron(III), completing the oxidation of EDOT to PEDOT. In turn, iron(III) ions are regenerated due to the presence of hydrogen peroxide in the medium. The experimental observations also indicate that hydrogen peroxide is very important to maintain the spherical morphology and to prevent the droplet coalescence [27].

TEM micrographs of the synthesized nanoparticles are shown in Figure 2. The increase of the molar ratio EDOT:FeTos results in a greater aggregation of the particles. However, the stability of the suspension was not affected by this partial aggregation, with the samples being stable even after one month. The particle size of the PEDOT nanoparticles was determined by dynamic light scattering (DLS). The sizes of nanoparticles prepared with EDOT:FeTos molar ratios of 1:1, 1:1.5, and 1:2 were 180 ± 10 , 260 ± 20 , and 490 ± 70 nm, respectively. These results are in agreement with the observations in TEM images, which point out a higher formation of aggregates at higher contents of oxidant. The statistical treatment of TEM micrographs for the sample obtained at the lowest molar ratio confirms a size distribution centered around 180 nm.

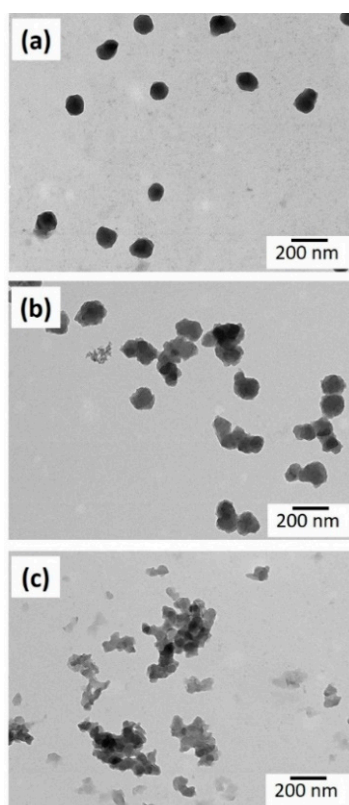


Figure 2. TEM images of particles prepared with EDOT:FeTos ratios of (a) 1:1, (b) 1:1.5, and (c) 1:2.

The assembly of PEDOT nanoparticles and CNT layers is controlled by the electrostatic interaction of PDADMAC (cationic polyelectrolyte) and DOC (anionic surfactant). It is thus important to know the surface charge of the nanoparticles and the CNTs. The zeta potential of the synthesized nanoparticles was $+19.3 \pm 0.5$ mV. This positive value indicates that PEDOT nanoparticles are positively charged due to the presence of PDADMAC at the surface. For the prepared CNTs dispersions, the zeta potential was -29.6 ± 0.3 mV, which is consistent with the functionalization with DOC. The zeta potential values confirm that the assembly of PEDOT–CNTs bilayers can be carried out by means of LbL deposition, through electrostatic interactions of the two components.

After preparation of the films by the drop-casting method (approximate thickness of $1.5 \pm 0.2 \mu\text{m}$), their thermoelectric properties were measured. Figure 3 shows the variation of the electrical conductivity, Seebeck coefficient, and power factor as a function of the EDOT:FeTos molar ratio and the type of CNTs. As expected, the electrical conductivity increases with the FeTos content, since the oxidation level of PEDOT is higher when the EDOT:FeTos molar ratio increases. The Seebeck coefficient is also affected by the oxidant content. Normally, the evolution of the Seebeck coefficient is opposite to the electrical conductivity when the oxidation level of conducting polymers changes [28–30]. However, in this particular case, both parameters, electrical conductivity and Seebeck coefficient, follow the same trend. This fact can be explained by looking at the nanostructure of the particles. The interconnection degree between particles is greater for an EDOT:FeTos ratio of 1:2 than for 1:1, as a result of the tendency of the particles to agglomerate and create a more connected path, which improves the charger transport across the film. The electrical conductivity of SWCNTs is higher than for the other CNTs (Figure 3b), which is related to the electronic structure. In the case of DWCNTs, which are a subset of MWCNTs, there are four unique permutations of inner@outer wall combinations: semi@semi, metal@metal, semi@metal, and metal@semi [31]. Taking into account that the conductivity of semiconductor nanotubes is smaller, if we extrapolate these combinations to MWCNTs, the probability of having semiconductor nanotubes increases and, therefore, the conductivity decreases [32–34]. The Seebeck coefficient reached a value of $55 \mu\text{V K}^{-1}$ in agreement with previous work [35].

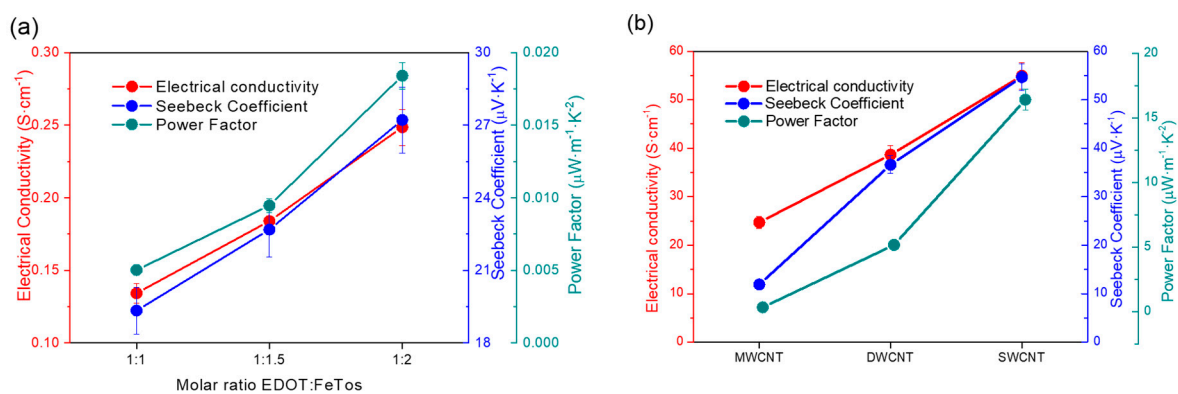


Figure 3. Variation of electrical conductivity, Seebeck coefficient, and power factor: (a) as a function of the molar ratio EDOT:FeTos and (b) as a function of the type of carbon nanotubes.

The assembly of the PEDOT and CNTs layers was performed according to the procedure shown in Figure 1b, using MWCNT, DWCNT, and SWCNT with the different EDOT:FeTos molar ratios and different numbers of bilayers (10–60 bilayers). Figure 4 shows profilometry measurements of the different systems studied. Initially, the thickness of the film increases progressively up to ca. $2 \mu\text{m}$ when increasing the number of bilayers. Then, the thickness rises rapidly to $3.5\text{--}4 \mu\text{m}$ with only 10 bilayers more. This fact is anomalous and can be explained by an interdiffusion phenomenon between PDADMAC and DOC. Both charged molecules interact with each other due to the high concentration, forming agglomerates on the surface of the film [36]. This observation is in agreement with the SEM and TEM micrographs of the film cross-sections, presented in Figure 5.

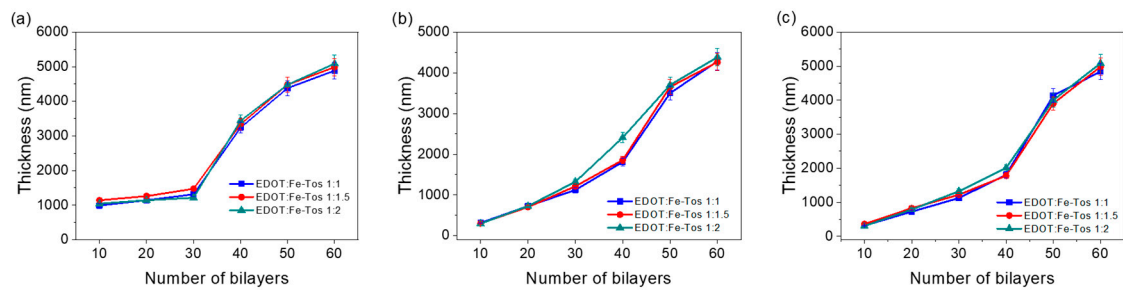


Figure 4. Profilometry measurements as a function of the number of bilayers for (a) MWCNT–PEDOT nanoparticles, (b) DWCNT–PEDOT nanoparticles, and (c) SWCNT–PEDOT nanoparticles.

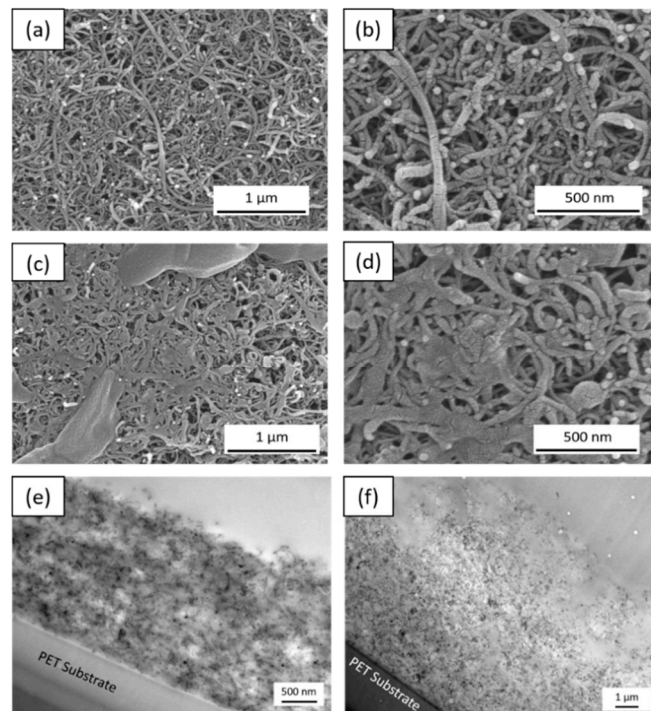


Figure 5. SEM and TEM cross-section images of (a,b,e) 30 bilayers of MWCNT-PEDOT and (c,d,f) 40 bilayers of MWCNT-PEDOT.

For 30 bilayers (Figure 5a,b), PEDOT nanoparticles are uniformly distributed over the MWCNTs fibers due to the electrostatic interactions between PDADMAC and DOC. The morphology of these nanoparticles remains essentially spherical. However, for 40 bilayers (Figure 5c,d), agglomerates of PEDOT nanoparticles that cover the nanotubes are observed on the surface of the films. These agglomerates increase the film thickness and the proportion of insulating material at the surface. TEM images of the cross-section of 30 and 40 bilayer films using MWCNTs (Figure 5e,f) indicate again an interdiffusion phenomenon, with a noticeable increase of the film thickness. Figure 5f shows that the formation of the first layers of MWCNT–PEDOT nanoparticles proceeds uniformly, but when reaching about 2 μm, the film formation is less uniform, with a much greater amount of insulating material. Photographs of the films obtained with 10 to 60 bilayers, shown in Figure 6, demonstrate how the homogeneity of the film is gradually lost with increasing the number of bilayers.

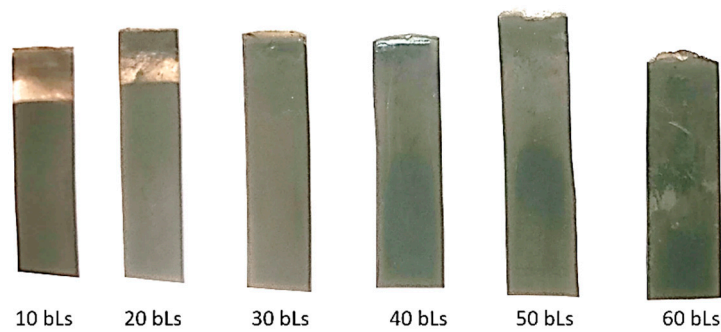


Figure 6. Films with different number of bilayers (bLs) of PEDOT-MWCNT.

Figure 7 shows the thermoelectric parameters of the different systems as a function of the number of bilayers. The electrical conductivity increases until reaching 30 (in case of MWCNTs) or 40 bilayers (for DWCNTs and SWCNTs). Then, it decreases due to the interdiffusion phenomenon between PDADMAC and DOC, which increases the proportion of insulating material on the surface of the film, as already described above. On the other hand, according to the Van der Pauw method for measuring electrical conductivity, an increase in thickness leads to a decrease in electrical conductivity [37]. The best result of electrical conductivity, with values up to 35 S cm^{-1} , was obtained by using SWCNTs with PEDOT nanoparticles with an EDOT:Fe-Tos molar ratio of 1:2. The Seebeck coefficient has a similar tendency: it increases until 40 bilayers and then it decreases because the agglomerates of PDADMAC and DOC hinder the passage of the current produced by the difference of temperature. Using SWCNTs with PEDOT nanoparticles at EDOT:FeTos molar ratio of 1:2, the Seebeck coefficient reached a maximum of $145 \mu\text{V K}^{-1}$, higher than water-based polymer emulsion methods containing SWCNTs and PEDOT:PSS [9]. As the electrical conductivity increases with the number of bilayers, the Seebeck coefficient remains relatively constant. This decoupling between the Seebeck coefficient and the electrical conductivity does not occur in conventional thermoelectric bulk materials, which is explained by the fact that, in the composites with CNT, the thermal conductivity decreases and the electrical conductivity is improved [9]. Finally, the power factor follows the same trend as the electrical conductivity: it increases progressively until 30 (MWCNTs) or 40 bilayers (DWCNTs and SWCNTs) and then sharply decreases. The best power factor was $72 \mu\text{W m}^{-1} \text{ K}^{-2}$, achieved by using SWCNTs with PEDOT nanoparticles at an EDOT:FeTos molar ratio of 1:2. This value is three orders of magnitude higher than the power factor of pristine PEDOT nanoparticles prepared at the same molar ratio. We suggest that this fact might be explained by the synergistic π - π interaction between the benzene ring of the CNTs and the aromatic ring of the PEDOT, which induces a greater ordering of the polymeric chain thus improving thermoelectric properties. Interestingly, this value is also higher than previously reported ones for different PEDOT-based materials, including polymer emulsions of PEDOT:PSS/SWCNT/Arabic-gum [9], PEDOT:PSS/SWCNT deposited by spin-casting [38], composites by in situ polymerization of EDOT in the presence of MWCNT and graphene stabilized by PSS [39], and flexible thermoelectric composite films of polypyrrole and carbon nanotubes [40].

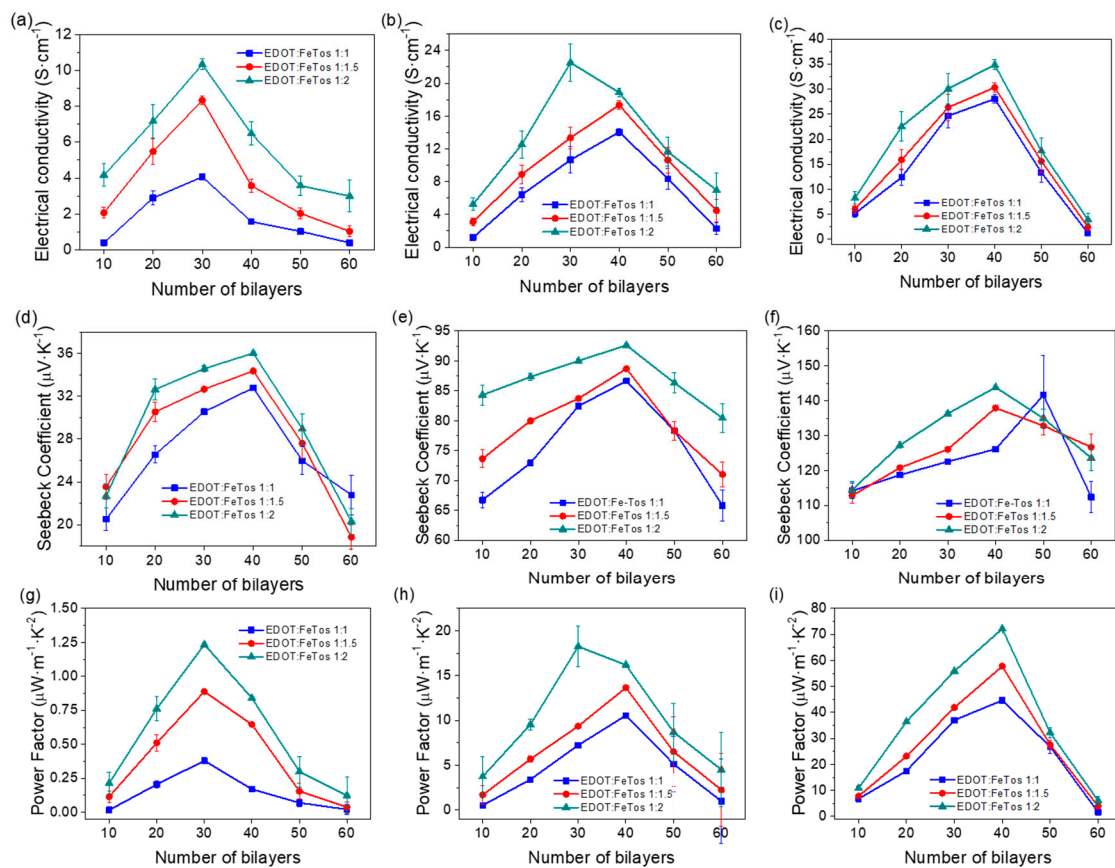


Figure 7. Electrical conductivity of (a) MWCNT–PEDOT nanoparticles, (b) DWCNT–PEDOT nanoparticles and (c) SWCNT–PEDOT nanoparticles. Seebeck coefficient of (d) MWCNT–PEDOT nanoparticles, (e) DWCNT–PEDOT nanoparticles and (f) SWCNT–PEDOT nanoparticles. Power Factor of (g) MWCNT–PEDOT nanoparticles, (h) DWCNT–PEDOT nanoparticles and (i) SWCNT–PEDOT nanoparticles as a function of the number of bilayers.

Finally, the flexible behavior of the prepared films was determined by measuring the electrical conductivity by performing up to 3000 bends on a cylinder with a radius of 2 cm. Figure 8 shows the flexible behavior of the film of 20 bilayers based on SWCNT and PEDOT nanoparticles with an EDOT:FeTos molar ratio of 1:2. The electrical conductivity remains practically constant, decreasing only 6% after 3000 bends, which indicates that there is no layer delamination or decomposition of the films during the bending. The observations demonstrate that multilayer materials based on carbon nanotubes and nanostructured conducting polymers are potentially suitable materials for flexible thermoelectric devices.

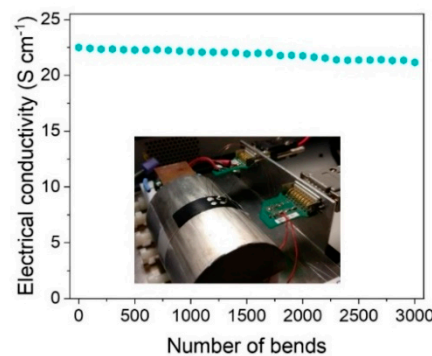


Figure 8. Electrical conductivity as a function of the number of bends for a film with the film of 20 bilayers based on SWCNT and PEDOT nanoparticles.

4. Conclusions

Hybrid thermoelectric flexible films with high Seebeck coefficient were prepared through layer-by-layer (LbL) assembly by using as building blocks PEDOT nanoparticles functionalized with PDADMAC and different types of carbon nanotubes functionalized with DOC. Depending on the EDOT:FeTos molar ratio used during the nanoparticle synthesis, the electrical conductivity and the Seebeck coefficient increase in parallel to the molar ratio. The maximum power factor was achieved at an EDOT:FeTos molar ratio of 1:2. Thanks to the electrostatic interaction of PDADMAC with DOC, the layers of the films grew homogeneously. However, when the film reached 30 or 40 bilayers (for MWCNTs or DWCNTs/SWCNTs, respectively) an interdiffusion phenomenon of the components appeared, as observed by SEM and TEM, and the proportion of insulating material increased. This fact influence negatively the thermoelectric properties and the homogeneity, so that we conclude that 30 and 40 bilayers are the limit for these materials. The maximum power factor of the hybrid flexible films was achieved for 40 bilayers at an EDOT:FeTos molar ratio of 1:2 and SWCNT. According to the obtained results, PEDOT nanoparticles with carbon nanotubes, especially SWCNTs, are very suitable candidates to make flexible films for thermoelectric applications.

Author Contributions: Conceptualization, M.C., C.M.G. and R.M.-E.; methodology, all authors; formal analysis, C.M.G. and R.M.-E.; investigation, J.F.S.-C. and M.C.; data curation, J.F.S.-C. and M.C.; writing—original draft preparation, J.F.S.-C. and R.M.-E.; writing—review and editing, all authors; supervision, A.C., C.M.G., and R.M.-E.; funding acquisition, A.C., C.M.G., and R.M.-E. All authors have read and agreed to the published version of the manuscript.

Funding: This research was funded by the Spanish Ministry of Science, Innovation and Universities through grants no. RTI2018-093711-B-I00 and MAT2015-63955-R.

Acknowledgments: J.F.S.-C and R.M.-E. acknowledge the financial support from the Spanish Ministry of Science, Innovation and Universities through the FPU17/01414 training program and a Ramón y Cajal grant (Grant RYC-2013-13451), respectively.

Conflicts of Interest: The authors declare no conflict of interest.

References

1. Culebras, M.; Gómez, C.M.; Cantarero, A. Review on Polymers for Thermoelectric Applications. *Materials* **2014**, *7*, 6701–6732. [[CrossRef](#)] [[PubMed](#)]
2. Zebarjadi, M.; Esfarjani, K.; Dresselhaus, M.S.; Ren, Z.F.; Chen, G. Perspectives on thermoelectrics: from fundamentals to device applications. *Energy Environ. Sci.* **2012**, *5*, 5147–5162. [[CrossRef](#)]
3. Dubey, N.; Leclerc, M. Conducting polymers: Efficient thermoelectric materials. *J. Polym. Sci. B Polym. Phys.* **2011**, *49*, 467–475. [[CrossRef](#)]
4. Huewe, F.; Steeger, A.; Kostova, K.; Burroughs, L.; Bauer, I.; Strohriegl, P.; Dimitrov, V.; Woodward, S.; Pflaum, J. Low-Cost and Sustainable Organic Thermoelectrics Based on Low-Dimensional Molecular Metals. *Adv. Mater.* **2017**, *29*, 1605682. [[CrossRef](#)]
5. Wei, Q.; Mukaida, M.; Kirihara, K.; Naitoh, Y.; Ishida, T. Recent Progress on PEDOT-Based Thermoelectric Materials. *Materials* **2015**, *8*, 732–750. [[CrossRef](#)]
6. Culebras, M.; Gómez, C.M.; Cantarero, A. Enhanced thermoelectric performance of PEDOT with different counter-ions optimized by chemical reduction. *J. Mater. Chem. A* **2014**, *2*, 10109–10115. [[CrossRef](#)]
7. Culebras, M.; Uriol, B.; Gómez, C.M.; Cantarero, A. Controlling the thermoelectric properties of polymers: application to PEDOT and polypyrrole. *Phys. Chem. Chem. Phys.* **2015**, *17*, 15140–15145. [[CrossRef](#)]
8. Yu, C.; Kim, Y.S.; Kim, D.; Grunlan, J.C. Thermoelectric Behavior of Segregated-Network Polymer Nanocomposites. *Nano Lett.* **2008**, *8*, 4428–4432. [[CrossRef](#)]
9. Kim, D.; Kim, Y.; Choi, K.; Grunlan, J.C.; Yu, C. Improved Thermoelectric Behavior of Nanotube-Filled Polymer Composites with Poly (3, 4-ethylenedioxythiophene) Poly (styrenesulfonate). *ACS Nano* **2010**, *4*, 513–523. [[CrossRef](#)]
10. Fan, W.; Liang, L.; Zhang, B.; Guo, C.-Y.; Chen, G. PEDOT thermoelectric composites with excellent power factors prepared by 3-phase interfacial electropolymerization and carbon nanotube chemical doping. *J. Mater. Chem. A* **2019**, *7*, 13687–13694. [[CrossRef](#)]

11. Hiroshige, Y.; Ookawa, M.; Toshima, N. High thermoelectric performance of poly (2,5—dimethoxyphenylenevinylene) and its derivatives. *Synth. Met.* **2006**, *156*, 1341–1347. [[CrossRef](#)]
12. Oh, J.Y.; Shin, M.; Lee, J.B.; Ahn, J.-H.; Baik, H.K.; Jeong, U. Effect of PEDOT Nanofibril Networks on the Conductivity, Flexibility, and Coatability of PEDOT:PSS Films. *ACS Appl. Mater. Interfaces* **2014**, *6*, 6954–6961. [[CrossRef](#)] [[PubMed](#)]
13. Chung, S.-H.; Kim, D.H.; Kim, H.; Kim, H.; Jeong, S.W. Thermoelectric properties of PEDOT:PSS and acid—treated SWCNT composite films. *Mater. Today Commun.* **2019**, 100867.
14. Yao, Q.; Chen, L.; Zhang, W.; Liufu, S.; Chen, X. Enhanced Thermoelectric Performance of Single-Walled Carbon Nanotubes/Polyaniline Hybrid Nanocomposites. *ACS Nano* **2010**, *4*, 2445–2451. [[CrossRef](#)]
15. Culebras, M.; Igual-Muñoz, A.M.; Rodríguez-Fernández, C.; Gómez-Gómez, M.I.; Gómez, C.; Cantarero, A. Manufacturing Te/PEDOT Films for Thermoelectric Applications. *ACS Appl. Mater. Interfaces* **2017**, *9*, 20826–20832. [[CrossRef](#)]
16. Chen, X.; Dai, W.; Wu, T.; Luo, W.; Yang, J.; Jiang, W.; Wang, L. Thin Film Thermoelectric Materials: Classification, Characterization, and Potential for Wearable Applications. *Coatings* **2018**, *8*, 244. [[CrossRef](#)]
17. Cho, C.; Stevens, B.; Hsu, J.-H.; Bureau, R.; Hagen, D.A.; Regev, O.; Yu, C.; Grunlan, J.C. Completely Organic Multilayer Thin Film with Thermoelectric Power Factor Rivaling Inorganic Tellurides. *Adv. Mater.* **2015**, *27*, 2996–3001. [[CrossRef](#)]
18. Cho, C.; Wallace, K.L.; Tzeng, P.; Hsu, J.-H.; Yu, C.; Grunlan, J.C. Outstanding Low Temperature Thermoelectric Power Factor from Completely Organic Thin Films Enabled by Multidimensional Conjugated Nanomaterials. *Adv. Energy Mater.* **2016**, *6*, 1502168. [[CrossRef](#)]
19. Cho, C.; Culebras, M.; Wallace, K.L.; Song, Y.; Holder, K.; Hsu, J.-H.; Yu, C.; Grunlan, J.C. Stable n-type thermoelectric multilayer thin films with high power factor from carbonaceous nanofillers. *Nano Energy* **2016**, *28*, 426–432. [[CrossRef](#)]
20. Yamamuro, H.; Hatsuta, N.; Wachi, M.; Takei, Y.; Takashiri, M. Combination of Electrodeposition and Transfer Processes for Flexible Thin—Film Thermoelectric Generators. *Coatings* **2018**, *8*, 22. [[CrossRef](#)]
21. Yamamuro, H.; Takashiri, M. Power Generation in Slope-Type Thin-Film Thermoelectric Generators by the Simple Contact of a Heat Source. *Coatings* **2019**, *9*, 63. [[CrossRef](#)]
22. Yao, C.-J.; Zhang, H.-L.; Zhang, Q. Recent Progress in Thermoelectric Materials Based on Conjugated Polymers. *Polymers* **2019**, *11*, 107. [[CrossRef](#)] [[PubMed](#)]
23. Andersson, H.; Šuly, P.; Thungström, G.; Engholm, M.; Zhang, R.; Mašlík, J.; Olin, H. PEDOT: PSS Thermoelectric Generators Printed on Paper Substrates. *J. Low Power Electron. Appl.* **2019**, *9*, 14. [[CrossRef](#)]
24. Li, J.; Du, Y.; Jia, R.; Xu, J.; Shen, S.Z. Thermoelectric Properties of Flexible PEDOT:PSS/Polypyrrole/Paper Nanocomposite Films. *Materials* **2017**, *10*, 780. [[CrossRef](#)]
25. Hong, C.T.; Kang, Y.H.; Ryu, J.; Cho, S.Y.; Jang, K.-S. Spray-printed CNT/P3HT organic thermoelectric films and power generators. *J. Mater. Chem. A* **2015**, *3*, 21428–21433. [[CrossRef](#)]
26. Naghdi, S.; Rhee, K.Y.; Hui, D.; Park, S.J. A Review of Conductive Metal Nanomaterials as Conductive, Transparent, and Flexible Coatings, Thin Films, and Conductive Fillers: Different Deposition Methods and Applications. *Coatings* **2018**, *8*, 278. [[CrossRef](#)]
27. Culebras, M.; Serrano-Claumarchirant, J.F.; Sanchis, M.J.; Landfester, K.; Cantarero, A.; Gómez, C.M.; Muñoz-Espí, R. Conducting PEDOT Nanoparticles: Controlling Colloidal Stability and Electrical Properties. *J. Phys. Chem. C* **2018**, *122*, 19197–19203. [[CrossRef](#)]
28. Zou, Y.; Huang, D.; Meng, Q.; Di, C.-A.; Zhu, D. Correlation between Seebeck coefficient and transport energy level in poly(3-hexylthiophene). *Organ. Electron.* **2018**, *56*, 125–128. [[CrossRef](#)]
29. Russ, B.; Glauddell, A.; Urban, J.J.; Chabiny, M.L.; Segalman, R.A. Organic thermoelectric materials for energy harvesting and temperature control. *Nat. Rev. Mater.* **2016**, *1*, 16050. [[CrossRef](#)]
30. Bubnova, O.; Khan, Z.U.; Malti, A.; Braun, S.; Fahlman, M.; Berggren, M.; Crispin, X. Optimization of the thermoelectric figure of merit in the conducting polymer poly (3,4-ethylenedioxythiophene). *Nat. Mater.* **2011**, *10*, 429. [[CrossRef](#)]
31. Blackburn, J.L.; Ferguson, A.J.; Cho, C.; Grunlan, J.C. Carbon-Nanotube-Based Thermoelectric Materials and Devices. *Adv. Mater.* **2018**, *30*, 1704386. [[CrossRef](#)] [[PubMed](#)]
32. Moore, K.E.; Tune, D.D.; Flavel, B.S. Double-Walled Carbon Nanotube Processing. *Adv. Mater.* **2015**, *27*, 3105–3137. [[CrossRef](#)] [[PubMed](#)]

33. Romero, H.E.; Sumanasekera, G.U.; Mahan, G.D.; Eklund, P.C. Thermoelectric power of single-walled carbon nanotube films. *Phys. Rev. B* **2002**, *65*, 205410. [[CrossRef](#)]
34. Hayashi, D.; Nakai, Y.; Kyakuno, H.; Yamamoto, T.; Miyata, Y.; Yanagi, K.; Maniwa, Y. Improvement of thermoelectric performance of single-wall carbon nanotubes by heavy doping: Effect of one-dimensional band multiplicity. *Appl. Phys. Express* **2016**, *9*, 125103. [[CrossRef](#)]
35. Tambasov, I.A.; Voronin, A.S.; Evsevskaya, N.P.; Volochaev, M.N.; Fadeev, Y.V.; Krylov, A.S.; Aleksandrovskii, A.S.; Luk'yanenko, A.V.; Abelyan, S.R.; Tambasova, E.V. Structural and Thermoelectric Properties of Optically Transparent Thin Films Based on Single-Walled Carbon Nanotubes. *Phys. Solid State* **2018**, *60*, 2649–2655. [[CrossRef](#)]
36. Culebras, M.; Cho, C.; Kreckler, M.; Smith, R.; Song, Y.; Gómez, C.M.; Cantarero, A.; Grunlan, J.C. High Thermoelectric Power Factor Organic Thin Films through Combination of Nanotube Multilayer Assembly and Electrochemical Polymerization. *ACS Appl. Mater. Interfaces* **2017**, *9*, 6306–6313. [[CrossRef](#)] [[PubMed](#)]
37. van der Pauw, L.J. A method of measuring specific resistivity and Hall effect of discs of arbitrary shape. *Philips Res. Repts.* **1958**, *13*, 1–9.
38. Song, H.; Liu, C.; Xu, J.; Jiang, Q.; Shi, H. Fabrication of a layered nanostructure PEDOT:PSS/SWCNTs composite and its thermoelectric performance. *RSC Adv.* **2013**, *3*, 22065–22071. [[CrossRef](#)]
39. Hong, C.T.; Lee, W.; Kang, Y.H.; Yoo, Y.; Ryu, J.; Cho, S.Y.; Jang, K.-S. Effective doping by spin-coating and enhanced thermoelectric power factors in SWCNT/P3HT hybrid films. *J. Mater. Chem. A* **2015**, *3*, 12314–12319. [[CrossRef](#)]
40. Li, J.; Du, Y.; Jia, R.; Xu, J.; Shen, S.Z. Flexible Thermoelectric Composite Films of Polypyrrole Nanotubes Coated Paper. *Coatings* **2017**, *7*, 211. [[CrossRef](#)]



© 2019 by the authors. Licensee MDPI, Basel, Switzerland. This article is an open access article distributed under the terms and conditions of the Creative Commons Attribution (CC BY) license (<http://creativecommons.org/licenses/by/4.0/>).